HHS Public Access

Author manuscript

ACS Appl Mater Interfaces. Author manuscript; available in PMC 2021 July 01.

Published in final edited form as:

ACS Appl Mater Interfaces. 2020 July 01; 12(26): 29056–29065. doi:10.1021/acsami.0c05792.

Liquid Crystal Emulsions that Intercept and Report on Bacterial Quorum Sensing

Benjamin J. Ortiz[1,†], **Michelle E. Boursier**[2,§], **Kelsey L. Barrett**[3], **Daniel E. Manson**[2], **Daniel Amador-Noguez**[3], **Nicholas L. Abbott**[1,‡], **Helen E. Blackwell**[2], **David M. Lynn**[1,2]

[1]Dept. of Chemical and Biological Engineering, Univ. of Wisconsin–Madison, 1415 Engineering Dr., Madison, WI 53706

[2]Dept. of Chemistry, Univ. of Wisconsin–Madison, 1101 University Ave., Madison, WI 53706, USA

[3]Dept. of Bacteriology, Univ. of Wisconsin–Madison, 1550 Linden Dr., Madison, WI 53706

Abstract

We report aqueous emulsions of thermotropic liquid crystals (LCs) that can intercept and report on the presence of *N*-acyl-L-homoserine lactones (AHLs), a class of amphiphile used by many pathogenic bacteria to regulate quorum sensing (QS), monitor population densities, and initiate group activities including biofilm formation and virulence factor production. The concentration of AHL required to promote 'bipolar' to 'radial' transitions in micrometer-scale droplets of the nematic LC 4'-pentyl-cyanobiphenyl (5CB) decreases with increasing carbon number in the acyl tail, reaching a threshold concentration of 7.1 μM for 3-oxo-C12-AHL, a native QS signal in the pathogen *Pseudomonas aeruginosa*. The LC droplets in these emulsions also respond to biologically relevant concentrations of the biosurfactant rhamnolipid, a virulence factor produced by communities of *P. aeruginosa* exclusively under the control of QS. Systematic studies using bacterial mutants support the conclusion that these emulsions respond selectively to the production of rhamnolipid and AHLs, and not to other products produced by bacteria at lower (sub-quorate) population densities. Finally, these emulsions remain configurationally stable in growth media, enabling them to be deployed either in bacterial supernatants or *in situ* in bacterial cultures to eavesdrop on QS and report on changes in bacterial group behavior that can be detected in real time using polarized light. Our results provide new tools to detect and report on bacterial QS and virulence and a materials platform for the rapid and *in situ* monitoring of bacterial communication and resulting group behaviors in bacterial communities.

Graphical Abstract

(H.E.B.) blackwell@chem.wisc.edu; (D.M.L.) dlynn@engr.wisc.edu.
†Current address: Abbvie, Inc., 1 N. Waukegan Road, North Chicago, IL 60064
§Current address: Amgen, Inc., 1 Amgen Center Dr., Thousand Oaks, CA 91320
‡Current address: Dept. of Chemical and Biomolecular Engineering, Cornell Univ., Ithaca, NY 14853

Supporting Information. Additional information on bacterial strains, characterization of LC droplets and culture supernatants, and the synthesis of HAA (PDF). This material is available free of charge via the Internet.

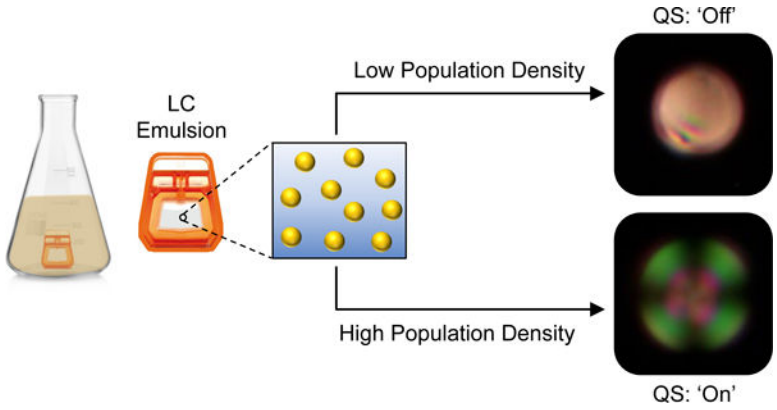

Keywords

Liquid crystals; amphiphiles; rhamnolipid; emulsions; bacteria; sensing

Introduction

Many common bacteria coordinate group behaviors and adapt to changing environments using a process known as quorum sensing (QS). This cell-cell communication process is controlled by the production and dissemination of small chemical signals that are 'shared' between cells in a population of bacteria.[1,2] In general, the concentration of these signals increases proportionally with the size of the bacterial population until a threshold density of cells (or a 'quorum') is reached, at which point QS signal-receptor binding initiates changes in gene expression that lead to changes in group behaviors, including motility,[3] toxin production,[2] and biofilm formation.[4] Several of the most common human, animal, and plant pathogens use QS to control virulence (*i.e.,* initiate infections)[1,2] or form biofilms that are detrimental in medical, industrial, and environmental settings (*i.e.,* surface fouling).[4] The development of strategies that can inhibit QS, enable the monitoring of QS signals, or detect and report on outcomes of QS is, thus, a rapidly growing area of research and has the potential to have impacts in a broad range of contexts.[5–10]

The work reported here was motivated by the potential utility of approaches for the *in situ* monitoring of QS and its outcomes in pathogenic Gram-negative bacteria. Many of these bacteria use amphiphilic molecules as QS signals and produce other amphiphilic species once a quorum is reached.[3,10–12] The opportunistic pathogen *Pseudomonas aeruginosa*, for example, uses amphiphilic *N*-acyl-L-homoserine lactones (AHLs) to regulate QS, and produces a class of bio-surfactants called rhamnolipids as a virulence factor at high cell densities.[1,2] The L-homoserine lactone head group of AHLs is conserved among Gram-negative bacteria, but the aliphatic acyl chain of these signals can vary in both length and chemical structure (Figure 1).[13] *P. aeruginosa* produces two chemically distinct AHLs to regulate QS: a longer-tailed *N*-(3-oxo-dodecanoyl)-L-homoserine lactone (3-oxo-C12-AHL) and a shorter-tailed *N*-butanoyl-L-homoserine lactone (C4-AHL; Figure 1).[14] Past studies have reported methods for the quantification or sensing of AHLs using genetically engineered bacterial biosensors or a variety of analytical methods (*e.g.,* HPLC, MS, NMR,

or electrochemical- and fluorescence-based methods).[15–22] However, these approaches often require extraction and/or purification of AHLs from bacterial media prior to analysis, and they can be difficult to apply *in situ* for real-time monitoring of QS in bacterial cultures.

Recent reports reveal that the amphiphilic nature of AHLs permits them to aggregate or self-assemble in solution and at interfaces in ways that are similar to conventional surfactants and lipids.[11,12] For example, long-chained AHLs (*e.g.*, C10-AHL and longer homologs) have been observed to aggregate at sufficiently high concentrations to form micelles and vesicles in aqueous media.[11] In addition, AHLs have been reported to adsorb and assemble at air/water interfaces or insert into phospholipid membranes.[23–25] We reasoned that these behaviors could be leveraged to provide new bases for detecting, monitoring, and quantifying AHLs. Here, we report a conceptually straightforward, scalable, and materials-based strategy for the rapid, real-time, and *in situ* monitoring of AHLs and other amphiphilic products of QS produced by bacteria. Our approach exploits the stimuli-responsive behaviors of oil-in-water emulsions containing micrometer-scale droplets of thermotropic liquid crystals (LCs).

Past studies demonstrate that colloidal droplets of LCs suspended in water can respond to low- or high-molecular weight amphiphiles that adsorb at the aqueous/LC interface and promote changes in the orientation of the LC that can be readily observed using polarized light.[26–33] These LC-emulsions are easy to prepare and enable the rapid and label-free detection of a range of amphiphilic species, including lipids,[26,28,30] surfactants,[27,31] peptides,[32] and proteins,[33] with sensitivities that depend on the concentration and the structure of the amphiphile. This approach can be remarkably sensitive; past work has reported the detection of Lipid A, a six-tailed glycolipid component of bacterial endotoxin, at levels as low as 1 pg/mL in water.[28] Many other one- and two-tailed surfactants and lipids promote LC ordering transitions at concentrations in the range of 10–100 μg/mL.[28,29,34] In general, these LC droplets can be deployed in aqueous environments as free-floating sensors, or they can be encapsulated in polymer capsules to enhance colloidal stability in complex environments or immobilize them on surfaces.[34–37] This latter approach permits the design of plastic ‘test strips’ that could be used as a basis for the detection of environmental agents using a simple light microscope.[35,36]

This study sought to determine whether bacterial AHLs, and products under their control, could trigger ordering transitions in LC emulsions. We report that AHLs can adsorb at aqueous/LC interfaces and trigger rapid ‘bipolar-to-radial’ transitions in LC droplets that can be readily observed using polarized light microscopy and, at larger scales, quantified using flow cytometry. We also found that this approach can be used to readily detect and report the presence of bacterial rhamnolipids produced by *P. aeruginosa*. These LC emulsions remain stable in bacterial culture media, permitting them to be used to detect AHLs and rhamnolipid in bacterial supernatants or be deployed *in situ* to report the presence of these products in bacterial cultures. Our results provide new tools for the interception, detection, and reporting of QS regulators and products that are unique to or diagnostic of bacterial communities, and thus provide guidance for the development of new approaches to the rapid and *in situ* monitoring of bacterial populations.

Results and Discussion

AHLs and Rhamnolipids Promote Bipolar-to-Radial Transformations in LC Droplet Emulsions

Bacterial AHLs with long aliphatic acyl tails possess non-ionic amphiphilic structures and have been reported to exhibit behaviors characteristic of conventional surfactants and lipids, including the ability to self-assemble in solution and adsorb at interfaces.[11,12,23–25] It was not clear at the outset of these studies, however, whether AHLs would adsorb preferentially at aqueous/LC interfaces, or whether adsorption would occur in a manner sufficient to promote changes in the orientation of the LC droplets (*e.g.,* from 'bipolar' to 'radial' configurations that can be readily observed using polarized light). We thus performed a series of experiments to determine the influence of AHL concentration and head/tail group structure on the optical configurations of microscale droplets of the model nematic LC 4-cyano-4'-pentylbiphenyl (5CB) dispersed in PBS. For these studies, we selected a series of naturally occurring and common AHLs with acyl chains ranging from 4 to 12 carbons (Figure 1 and Table 1, below).[38,39] This series included 3-oxo-C12-AHL and C4-AHL, the native AHL signals of *P. aeruginosa*. To understand how changes in head group structure could affect the anchoring of the LC, we also included AHLs having different oxidation states at the third carbon of the acyl chain and a hydrolyzed, ring-opened form of 3-oxo-C12-AHL containing an ionizable homoserine group (referred to as 3-oxo-C12-HS; Figure 1). Hydrolysis of the AHL head group occurs naturally in aqueous solution, and hydrolyzed AHL is present, albeit QS-inactive, in bacterial cultures.[40] 3-oxo-C12-HS was thus also included here to understand whether this byproduct of QS could also be used as a marker to monitor bacterial populations. Finally, we also examined rhamnolipid and 3-(3-hydroxyalkanoyloxy)alkanoic acid (HAA), an amphiphilic species produced by *P. aeruginosa* as a precursor during rhamnolipid biosynthesis.[41]

We began by characterizing the influence of 3-oxo-C12-AHL on the anchoring of microscale droplets of LC in defined aqueous buffer. We prepared emulsions of 5CB in PBS and used polarized light microscopy and flow cytometry to characterize transitions in the LC droplets from 'bipolar' to 'radial' configurations.[27,42] Droplets of 5CB suspended in PBS exhibit so-called 'bipolar' configurations that have the diagnostic appearance shown in Figure 2B and 2C when viewed by bright-field or polarized light microscopy.[32, 45] In bipolar droplets, the director of the LC is aligned tangentially to the surface, which results in two topological defects at opposite poles of the droplet; a cartoon illustrating the director profile in a bipolar LC droplet is shown in Figure 2A.[32, 45] Upon addition of 3-oxo-C12-AHL at a concentration of 50 μM, these bipolar droplets were observed to change rapidly (within 1–2 s) and uniformly (approximately all droplets in any random field of view) to a so-called 'radial' configuration exemplified by the images shown in Figures 2D and 2E. In radial droplets, the director of the LC is aligned normal to the surface, with a single defect at the center of the droplet (see Figure 2A).[32, 45] This bipolar-to-radial transition is consistent with results observed in past studies on LC droplets in contact with conventional surfactants, [27,29,31,42] and reveals that this non-ionic amphiphile can adsorb at aqueous/LC interfaces and trigger diagnostic changes in the optical properties of the LC droplets.

Bipolar-to-radial transitions in LC droplets can also be quantified using a standard lab flow cytometer equipped with side and forward light scattering detectors. This method permits rapid characterization of large populations of LC droplets (*e.g.*, 10,000 or more droplets).[27] This analytical approach exploits differences in the ways that light is scattered by bipolar and radial LC droplets, again owing to differences in their internal configurations. These differences give rise to distinct scattering profiles when the intensity of side scattering (SSC) is plotted against that of forward scattering (FSC).[27] Light scattering profiles arising from samples of bipolar droplets and radial droplets produced by the addition of 3-oxo-C12-AHL are shown in Figure S1, and are consistent with past studies on the characterization of surfactant-treated LC droplets.[27,30] Past studies have also established that FSC histograms can be used to quantify the percentage of radial LC droplets in samples that contain mixtures of both bipolar and radial droplets.[27] Accordingly, we used flow cytometry to characterize and quantify changes in the ordering of LC droplets upon exposure to 3-oxo-C12-AHL at concentrations ranging from 2 to 50 μM, which is in the range of AHL concentrations found in laboratory cultures of planktonic *P. aeruginosa*.[22]

Figure 3A shows results for each concentration of 3-oxo-C12-AHL tested expressed as the percentage of droplets present in the radial state—that is, the percentage of droplets in a sample observed to have undergone a ‘bipolar-to-radial’ transition—after treatment with AHL (see SI for details of this analysis). Inspection of these results reveals a clear dependence of the ordering of LC droplets on the concentration of 3-oxo-C12-AHL. We observed >90% of LC droplets to be in the radial state at concentrations of AHL at or above 15 μM. The percentage of radial droplets dropped to ~60% at 8 μM and ~10% at 4 μM; we observed no meaningful change in droplet configuration at 2 μM. This concentration dependence is similar to those observed in LC droplet transitions promoted by conventional surfactants, which have been reported to occur through a mechanism that involves the adsorption of amphiphiles at levels nearing droplet surface saturation coverage to promote the transition to radial droplets.[34] Conventional one- and two-tailed surfactants typically trigger these transitions at concentrations on the order of 10 μg/mL; other many-tailed amphiphiles trigger these transitions through defect-mediated mechanisms that occur at concentrations five orders of magnitude lower.[28–30]

To characterize structure/function relationships that could govern the triggering of bipolar-to-radial transitions by non-ionic AHLs, we conducted additional concentration-dependence experiments using the other AHLs and derivatives shown in Figure 1 in the presence of the LC droplets. The full set of concentration-dependence profiles using these additional compounds is shown in Figure S2. Table 1 summarizes key results and shows the minimum concentration of each AHL required to induce a change from the bipolar to the radial state in at least a 50% of the LC droplets in a given sample, a value we refer to from hereon as the BR_{50} (BR = bipolar-to-radial; these values were obtained from sigmoidal regressions of the data plotted in Figures 3 and S2; see Figure S3). These results reveal the longer-tailed AHLs, namely 3-oxo-C12-AHL, 3-OH-C12-AHL, and the ring-opened AHL derivative 3-oxo-C12-HS, to have BR_{50} values ranging from 7 to 20 μM. The small, but significant, difference between the BR_{50} for 3-oxo-C12-AHL (7.1 μM) and the values for 3-oxo-C12-HS and 3-OH-C12-AHL (20 and 16 μM) could arise from structural features that influence the interfacial density of these species through head group/head group interactions, as

demonstrated in studies on surfactant-induced ordering transitions at LC-aqueous interfaces.[43,44] For example, the carboxylic acid moiety in the head group of 3-oxo-C12-HS has a reported pKa of ~3, calculated from molecular structure studies,[11] suggesting that, in the conditions used here, it should be substantially ionized, leading to repulsive head group/head group interactions that could lead to lower interfacial areal density.

Decreasing the length of the acyl tail by two carbons lead to a 4-fold increase in BR_{50} from 20 and 16 μM for 3-oxo-C12-HS and 3-OH-C12-AHL to >72 μM for C10-AHL (Figures S2 and S3; Table 1). This trend was also observed when moving from C10-AHL to C8-AHL, which exhibited a BR_{50} value of > 360 μM. We note here, however, that the extent of the bipolar-to-radial transition promoted by C8-AHL did not continue to increase at higher concentrations, as was observed for all longer-tailed AHLs; this shorter-tailed AHL did not promote transformations above ~60% at concentrations up to at least 500 μM (Figure S2D). Finally, AHLs with shorter acyl tails (C6-AHL and C4-AHL) failed to trigger distinguishable levels of bipolar-to-radial transitions in LC droplets even at concentrations as high as 1 mM (Figures 3B, S2E–F, and Table 1). These structure-function trends are consistent with those of past studies demonstrating that longer aliphatic tail groups and high areal densities of adsorbed surfactant are generally needed to promote robust changes in LC anchoring.[43,45–47]

We also subjected rhamnolipid and its biosynthetic precursor HAA to these same droplet screening experiments (Figure 3C–D and Table 1). These experiments were conducted at biologically relevant concentrations of these amphiphiles ranging from 0.8 to 25 μg/mL. Our results reveal that rhamnolipids promote bipolar-to-radial transformations in LC droplets at BR_{50} values as low as ~6 μg/mL. We estimate this value to be in the range of about 7 to 20 μM (see SI for details describing the estimation of this range). HAA triggered threshold levels at a BR_{50} of 2.3 μg/mL (~8 μM). Overall, this range of threshold concentrations is similar to that determined for the three C12-AHL species and derivatives described above, suggesting that these different compounds promote changes in LC droplets configurations through a similar mechanism.

LC Droplets Respond to AHLs and Rhamnolipid Produced in Growing Bacterial Cultures

We next performed experiments to determine whether droplets of 5CB could respond to and report on the presence of AHLs and rhamnolipid produced by growing cultures of bacteria. For these experiments, we devised an experimental setup in which LC emulsions were enclosed in a laboratory dialysis cassette that could be placed directly into a bacterial culture flask (Figure 4A). This enabled us to expose small volumes and high concentrations of LC droplets to bacterial products produced in larger volumes of culture medium without diluting them or complicating analysis by microscopy or flow cytometry. For these proof-of-concept studies, we selected dialysis cassettes that allowed AHLs and rhamnolipid to diffuse over a period of 90 min, and that permitted extraction of LC emulsion samples by syringe for analysis. This approach also prevented the possibility of direct contact between the LC droplets and cells, which has also been reported to lead to bipolar-to-radial transitions in past studies.[26]

In a first series of experiments, we used cultures of the PAO1 wild-type strain of *P. aeruginosa*. Cultures were grown in LB medium with shaking at 37 °C, and dialysis cassettes were added at pre-determined time points during growth and stationary phases to characterize changes in the responses of the LC droplets. We note that the nematic-isotropic transition temperature ($T_{N,I}$) for 5CB is 35 °C—that is, at a temperature above 35 °C, 5CB undergoes a phase transition from the nematic LC phase to an isotropic oil that does not exhibit the optical birefringence necessary for detection.[48] Cultures were therefore cooled to ambient temperature (~25 °C) prior to adding the LC droplet-containing dialysis cassettes; the cassettes were incubated with cultures for 90 min, removed, and sampled for analysis by flow cytometry. As an aside, we note that LCs with $T_{N,I} > 35$ °C have also been demonstrated to form LC droplets that undergo bipolar-to-radial transformations.[27,36] Those additional LC formulations could also be used to further optimize experimental and analytical workflow.

Columns I and II of Figure 4B show the responses of LC droplets placed in flasks containing (I) LB medium or (II) cultures of the PAO1 strain of *P. aeruginosa* in LB medium at 6 h (white bars), 12 h (black bars), or 24 h (grey bars) after inoculation. These results reveal cultures of PAO1 to induce bipolar-to-radial transitions in the LC droplets, and that the percentage of radial droplets increases monotonically over 24 h from ~15% at 6 h of incubation to >90% at 24 h. In contrast, incubation with LB medium resulted in only ~5% of radial droplets at 24 h. These results are consistent with the production of AHLs by these bacterial communities and/or the production of rhamnolipid and HAA, but they do not rule out responses that could be triggered by other products produced during bacterial growth.

To further investigate the factors that lead to droplet response under these conditions, we performed otherwise identical experiments using three mutant strains of *P. aeruginosa* lacking genes critical to either QS or rhamnolipid biosynthesis (see Table S1 for strain information). Strain PAO1 Δ*lasI*, Δ*rhlI* is unable to produce either of its native AHL signals, 3-oxo-C12-AHL or C4-AHL. This strain is thus unable to produce QS-associated virulence factors, including rhamnolipid (a detailed schematic of the QS regulatory pathway in *P. aeruginosa* is shown in Figure S4).[49] Strain PAO1 Δ*rhlB* is unable to produce the rhamnosyltransferase enzyme required to synthesize rhamnolipids,[50] and strain PAO1 Δ*rhlA* is unable to produce the rhamnolipid precursor HAA (and, as result, cannot produce any downstream rhamnolipids).[51] The results of experiments using these three knockout strains are included in Figure 4.

Inspection of the results shown in Column III of Figure 4B reveals cultures of the PAO1 Δ*lasI*, Δ*rhlI* QS-knockout strain to promote bipolar-to-radial transitions at very low levels that are similar to that of LB medium alone (the percentage of radial droplets was < 7% at all points tested). This result suggests that the response of the LC droplets to the wild-type strain (Figure 4B; Column II) was the result of either a QS signal or a factor regulated by bacterial QS, and not a metabolite, component of cellular debris, or other factor resulting from bacterial growth or death. Experiments using the PAO1 Δ*rhlA* strain (Figure 4B; Column V) showed a substantial (~70%) decrease in the percentage of droplets present in the radial state. This strain is able to produce both C4-AHL, which did not trigger bipolar-to-radial transitions in the experiments reported above, and 3-oxo-C12-AHL, which did induce

bipolar-to-radial transformations, to regulate QS—but it is unable to produce either HAA or rhamnolipid. We therefore interpret the response of the LC droplets to this strain to result from levels of 3-oxo-C12-AHL (and, likely, also its hydrolyzed, ring-opened derivative product 3-oxo-C12-HS) that accumulate in the culture medium as bacterial population density increases. The addition of exogenous C4-AHL (200 μM) to cultures of the PAO1 Δ*lasI*, Δ*rhlI* strain, which has been shown to promote the production of rhamnolipid yielded a substantial increase in LC droplet response.[49] The percentage of radial droplets under these conditions (Figure 4B; Column IV) was similar (>90%) to that observed in the wild-type strain (Column II) and substantially higher than that observed in that strain in the absence of exogenous C4-AHL (~6%; see Column III). Because this strain does not produce 3-oxo-C12-AHL, and because the exogenously added C4-AHL itself does not promote radial transitions at this concentration, this result suggests that the production of rhamnolipid is also sufficient to produce a robust LC droplet response. Lastly, Column VI of Figure 4B shows the results of experiments using the PAO1 Δ*rhlB* strain, which can produce both 3-oxo-C12-AHL and HAA, but not rhamnolipid. The extents of radial transitions observed using this strain (>80% at 24 h) in comparison to those using the PAO1 Δ*rhlA* strain suggest that production of HAA alone can also promote robust LC droplet responses. We note that cell densities in all of these experiments were virtually identical across all strains at all time points tested (Figure S5), and that 5CB emulsions did not exhibit substantial toxicity to PAO1 cells (Figure S6), further supporting the view that transitions observed here were the result of excreted compounds associated with QS and not differences in metabolite concentration or other factors associated with cell growth.

We conclude on the basis of these results that (i) the LC droplets used in these experiments can respond to and report on concentrations of long-chain AHLs present in bacterial communities as well as rhamnolipid or amphiphilic rhamnolipid precursors that are produced once a quorum is reached, and (ii) the majority of the LC droplet response observed in the wild-type strain at 12 or 24 h is the result of rhamnolipid or HAA production (a comparison of Columns II and IV of Figure 4 reveals >85% of the response observed for the wild-type strain at 24 h to arise from the production of rhamnolipid; only a small part of this response (~15%) arises from the accumulation of 3-oxo-C12-AHL or its hydrolysis product). Notably, because rhamnolipid is a virulence factor that is only produced once a quorum is reached, these results suggest that these LC emulsions can be used to monitor bacterial cultures and distinguish between quorate and sub-quorate populations.

Finally, we performed additional analytical experiments to determine the concentrations of 3-oxo-C12-AHL and rhamnolipid produced by cultures of each of the *P. aeruginosa* strains used above and compare them to the values observed to promote bipolar-to-radial transformations in defined buffer. The results of those experiments are summarized in Figure S7 (see SI for additional detailed discussion of findings and implications arising from those studies). Overall, the results of those experiments are consistent with those shown in Figure 4 and provide additional support for the view that 3-oxo-C12-AHL, 3-oxo-C12-HS, and rhamnolipid produced in cultures of *P. aeruginosa* are responsible, either alone or in combination, for promoting ordering transitions in LC droplets.

Conclusions

QS signals are markers of not only the presence of bacteria, but also their population densities. Approaches to detect these markers could thus provide novel means by which to monitor of the growth and behaviors of bacterial communities. We have demonstrated that LC emulsions can respond to amphiphilic AHL signals that control QS in Gram-negative bacteria. We have also demonstrated that LC droplets undergo bipolar-to-radial transitions upon exposure to products generated specifically by quorate populations of bacteria. The concentration of AHLs required to promote these transitions decreases with increasing carbon number in the acyl tail, reaching a BR_{50} of 8 μM for 3-oxo-C12-AHL, a native QS signal in *P. aeruginosa*. This concentration range is within that observed in quorate populations of *P. aeruginosa*. Our results also reveal these droplets to respond to biologically relevant concentrations of rhamnolipid, an amphiphile produced by *P. aeruginosa* under the control of QS.

These LC droplets remain configurationally stable in bacterial culture media, permitting them to be used to detect the presence of AHL and rhamnolipid in bacterial supernatants or be deployed *in situ* to report the presence of these products in growing bacterial cultures. Systematic studies using mutant *P. aeruginosa* strains, with certain aspects of their QS system rendered non-functional, support the conclusion that these LC droplets respond selectively to the production of rhamnolipid and other amphiphiles involved in the regulation of QS, and not to other products produced by bacteria at lower sub-quorate densities. The proof-of-concept studies reported here provide new methods for the detection and monitoring of bacterial QS and the production of QS-associated goods using free-floating LC droplets that can be readily applied in aqueous environments. These methods could also be combined with approaches for the encapsulation and immobilization of LC droplets on surfaces to design sensor arrays or flexible test strips that could facilitate the rapid and *in situ* monitoring of bacterial communities in practical settings.

Materials and Methods

Materials.

The nematic thermotropic LC 4’-pentyl-cyanobiphenyl (5CB) was purchased from HCCH Jiangsu Hecheng Display Technology Co., Ltd (Jiangsu, China). Disposable culture tubes (12 x 75 mm) were purchased from VWR (West Chester, PA). Phosphate-buffered saline (PBS) concentrate (137 mM NaCl; 2.7 mM KCl; 10 mM phosphate) was obtained from Omnipur (EM Science, Gibbstown, NJ). Electrophoresis-grade sodium dodecyl sulfate (SDS) was purchased from Fisher Scientific (Pittsburgh, PA). Rhamnolipids, 90% pure (commercial mixture of glycolipids isolated from *P. aeruginosa*; see additional notes below) were purchased from AGAE Technologies (Corvallis, OR). Dialysis cassettes (10k MWCO, gamma irradiated, 0.5 mL) were purchased from ThermoFisher Scientific (Rockford, IL). Luria-Bertani medium, Lennox formulation (LB) was purchased from EMD Millipore (Burlington, MA). The native AHLs *N*-butanoyl-L-homoserine lactone (C4-AHL) and *N*-(3-oxo-dodecanoyl)-L-homoserine lactone (3-oxo-C12-AHL) were purchased from Cayman Chemical (Ann Arbor, MI) and Sigma-Aldrich (St. Louis, MO), respectively. The other AHLs and AHL derivatives examined in this study were synthesized according to our

previously reported methods.[52,53] A detailed description of the synthesis and characterization of 3-(3-hydroxyalkanoyloxy)alkanoic acid (HAA) is included in a separate Supplementary Methods section below.

General Considerations.

All absorbance measurements were made using 200 μL of solution in a clear 96-well microtiter plate (Costar 3370) using a Biotek Synergy 2 plate reader running Gen 5 software (version 1.05). Bacterial growth was monitored by measuring culture density *via* absorbance at 600 nm (OD_{600}). Bright-field and polarized light microscopy images were acquired using an Olympus IX71 inverted microscope (Waltham, MA) equipped with cross-polarizers (Olympus analyzer slider IX2-AN and condenser attachment IX-LWPO) and a binocular tube built-in Bertrand lens (Olympus U-BI90CT). Fields of view were recorded using an OPTO-EDU (Beijing, China) eyepiece camera model A59.2211 connected to a computer and controlled through ImageView imaging software version A30.2201. The percentage of 5CB droplets in the radial state within an emulsion sample was determined by flow cytometry measurements performed at room temperature using a BD FACSCalibur™ instrument. Assay data were analyzed using Microsoft Excel for Mac 2016, cytometry data were analyzed using FlowJo™ (v10), and graphs were created using GraphPad Prism (GraphPad Software version 7, San Diego CA, USA). Characterization of emulsion droplet density was performed at room temperature using a BD Accuri C6 flow cytometer. HPLC-MS/MS data analysis was performed using the MAVEN software (open-source)[54] and Thermo Xcalibur software packages (Waltham, MA). Unless otherwise noted, all AHL solutions were prepared by first dissolving AHL in DMSO and then diluting further to the desired concentration at 1% v/v DMSO.

We note that the commercially obtained rhamnolipids used in this study were isolated from *P. aeruginosa* as a mixture of congeners with different numbers of rhamnose sugar moieties (mono- and di-) linked to one or two molecules of hydroxy acid that differ in their aliphatic chain length, and that the composition of this mixture has been found to depend on various environmental factors, including nutrient source and growth conditions.[55–57] Several studies have found that the most abundant species are mono- and di-rhamnolipids containing one or two 8–10 α-hydroxy fatty acids.[57] However, in cases where estimates of molar concentrations of rhamnolipid were calculated from diluted stocks of commercial rhamnolipid provided in units of μg/mL, we opted to establish a boundary range of molar concentrations by assuming two hypothetical uniform compositions consisting entirely of either the lowest or the highest molecular weight rhamnolipid congeners found in rhamnolipid mixtures. The actual molar concentration of rhamnolipid prepared from the commercial mixtures used here would then lie somewhere within that calculated range.

Preparation of LC Emulsions and Characterization of LC Droplet Configuration.

LC-in-water emulsions were prepared using a procedure similar to that previously reported by Carter *et. al.*[30] Briefly, 6 μL of 5CB was added to a glass test tube containing 3 mL of a 10 μM SDS solution in PBS. The mixture was vortexed for 30 s at ~3000 rpm to yield a milky white emulsion and allowed to settle for 1 h. The emulsion was divided into aliquots of 50 μL that were subsequently diluted into 500 μL of aqueous solutions of either AHL or

rhamnolipid, prepared at pre-determined concentrations, to obtain final LC droplet densities of ~10,800 ± 900 droplets/μL. These mixtures were allowed to sit for at least 1 h before characterizing the LC droplets using polarized light microscopy or flow cytometry. For flow cytometry experiments, forward light scattering (FSC) was measured at a detection angle of 0° ± 15° for a minimum of 10,000 droplets pumped through the flow cytometer at a flow rate of 12 μL/min. Quantitative analysis of scattering plots to determine the percentage of droplets in the bipolar or radial configurations was performed using a previously reported procedure.[30,58]

BR_{50} calculation.

BR_{50} values, representing the minimum concentration of each analyte required to induce a change from the bipolar to the radial state in at least a 50% of the LC droplets in a given sample, were calculated by performing a sigmoidal regression fit with a Hill slope ≠ 1 to plots of the percentage of droplets transitioned from bipolar-to-radial vs. analyte concentration. Fits were calculated using GraphPad Prism (GraphPad Software Version 7.0, San Diego CA, USA) and the built-in non-linear regression model for dose-response curves with a variable Hill slope using the following equation:

$$Y = 100 \cdot \frac{X^{Hill\ slope}}{BR_{50}^{Hill\ slope} + X^{Hill\ slope}}$$

Bacterial Strains and Growth Conditions.

The *P. aeruginosa* strains used in this study were: PAO1 [wild-type; isolated by B. Holloway from a human wound],[59] PW6886 *(ΔrhlA)* [PAO1 rhlA-E08::ISphoA/hah; tetracycline resistant],[51] PAO1 *(ΔrhlB)* [PAO1 containing an unmarked, in-frame *rhlB* deletion],[50] and PAO-SC4 (Δ*lasI*,*ΔrhlI)* [PAO1 containing unmarked, in-frame *rhlI* and *lasI* deletions; a generous gift from E. P. Greenberg]. Bacteria were cultured in LB broth at 37 °C with shaking at 200 RPM unless otherwise noted. Freezer stocks for the bacterial strains were stored at −80 °C in LB with 25% glycerol. Spent media was collected at varying time points by centrifugation (3500 x*g*, 15 min) and stored at −80 °C until use.

Incubation of Bacteria with LC Droplets.

A 2 mL overnight culture of each *P. aeruginosa* strain was grown for 20 h in a sterile borosilicate glass test tube. A subculture was prepared by directly diluting overnight culture 1:100 in 75 mL of fresh LB medium. For the induction of rhamnolipid production in PAO-SC4 (Δ*rhlI ΔlasI)*, 150 μL of 100 mM BHL stock solution was added to yield a final concentration of 200 μM; DMSO alone (150 μL; 0.2% DMSO) was added to all other strains. Subcultures were grown for 6, 12, or 24 h. Cultures were then briefly chilled on ice. Prior to use, dialysis cassettes were equilibrated in LB medium according to the manufacturer's instructions. LC suspension (600 μL) was then added to the cassette, and the cassette was added to the chilled culture. Cultures were incubated at 20 °C with shaking for 1.5 h. Cassettes were then removed from culture, and the LCs were collected for analysis by flow cytometry.

Quantification of Rhamnolipid.

Rhamnolipid was quantified using the orcinol assay method described by Welsh *et al.* with the following modifications.[60] At time points of interest, 2 mL of culture was removed from the 75 mL subculture, and the cells were pelleted at 3500 x*g* for 15 min. A 1-mL aliquot of supernatant was removed, extracted, and characterized using the reported orcinol assay. The remaining supernatant was saved for quantification of AHL, as discussed below. Samples were background corrected using an LB negative control. Rhamnolipids were quantified using a rhamnose standard curve based on the assumption described by Pearson *et al.* that 1 g of rhamnose equals 2.5 g of rhamnolipid mixture.[49]

Characterization of Cell Viability.

LC-in-water emulsions were prepared as described above. Droplet density was estimated based on a calibration curve obtained from correlations between event counts/μL detected using a BD Accuri C6 flow cytometer and dilutions from stock LC-in-water emulsions (of at least three different dilutions). A sample with a droplet density of 20,000 events/μL was prepared from stock LC emulsion based on the estimated droplet density. Serial dilutions were performed from this LC emulsion. A 2 mL overnight culture of wild type *P. aeruginosa* PAO1 was grown for 20 h and plated in a 1:1 dilution with varying dilutions of LC droplets in a 96 well microtiter plate. Plates were incubated under static conditions for 1.5 h at either 37 °C or room temperature. Cell viability was quantified using BacTiter-Glo™ Microbial Cell Viability Assay (Promega Corporation) and normalized using a no-LC control.

Characterization of AHL Concentrations Using HPLC-MS/MS.

Cell-free supernatant was collected from each sample at 6, 12, and 24 h prior to addition of the dialysis cassette and stored at −80 °C until use. After thawing, the samples were diluted 1:10 in 10:90 methanol:water with 5 mM ammonium formate and 0.1% formic acid (any samples doped with C4-AHL, including C4-AHL standards, were diluted 1:100 in the same solvent). AHL concentrations were measured using external calibration curves. AHL standards were prepared in PBS immediately before use. Ring-opened (i.e., hydrolyzed lactone) AHL standards were prepared by incubating AHLs in 1M NaOH for 12 h at room temperature.

The method for HPLC-MS/MS analysis was adapted from that of Patel *et al.*[20] Aliquots totaling 2.5 μL of diluted supernatant samples were subjected to HPLC-MS/MS analysis. HPLC was performed on a Vanquish™ μHPLC system (Thermo Scientific) using a C18 reversed-phase column (1.7 μm particle size, 2.1 x 50 mm; Acquity UPLC BEH). Solvent A consisted of 10:90 methanol:water with 5 mM ammonium formate and 0.1% formic acid, and solvent B was 100% methanol. The gradient profile for chromatography was as follows: 100% solvent A for 1 min, linear increase in solvent B to 90% over 4 min, isocratic 90% solvent B for 5.5 min, and then equilibration with 100% solvent A for 2 min. The flow rate was constant at 0.2 mL/min. Compounds separated by HPLC were detected by heated electrospray ionization coupled to high-resolution mass spectroscopy (HESI-MS) (QExactive; Thermo Scientific). Analysis was performed in positive ionization mode. Settings for the ion source were: 10 aux gas flow rate, 35 sheath gas flow rate, 1 sweep gas flow rate, 4 μA spray current, 4 kV spray voltage, 320 °C capillary temperature, 300 °C

heater temperature, and 50 S-lens RF level. Nitrogen was used as the nebulizing gas by the ion trap source. The MS/MS method was designed to perform an MS1 full-scan (100 to 510 m/z, no fragmentation) together with a series of MS/MS scans (all-ion fragmentation) that divided the *m/z* range into partially overlapping windows of 40 *m/z* each. The MS1 full-scan provided data on $[M + H]^+$ pseudo-molecular ions, while the MS/MS scans provided corresponding (matched by retention time) fragmentation spectra, all obtained within a single chromatographic run. MS/MS scans (all-ion fragmentation) were centered at 160, 210, 245, 280, 315, 350, 385, 420, 455, 490 *m/z* using an isolation width of 40.0 *m/z*. Fragmentations were performed at 17.5, 35, and 52.5 NCE (normalized-collision energy). Mass resolution was set at 35000, AGC target was 1E6, and injection time was 40 ms.

Statistical Information.

All statistical test and sigmoidal regression fits were performed using GraphPad Prism (GraphPad Software Version 7.0, San Diego CA, USA). Statistical comparisons were evaluated using two-way analysis of variance (ANOVA) using Dunnett's post hoc test for multiple comparisons. The criterion used to accept statistical significance was a p value of less than 0.05. Data were generated by at least three independent experiments. Separate biological replicates were the result of three technical replicates.

Supplementary Material

Refer to Web version on PubMed Central for supplementary material.

Acknowledgment.

Financial support was provided by the NSF through a grant to the UW–Madison MRSEC (DMR-1720415) and the ONR (N00014-07-1-0255). We acknowledge the use of instrumentation supported by the NSF through the UW MRSEC. B.J.O. was supported by the Graduate Research Scholars program at UW-Madison and the NIH Chemistry-Biology Interface Training Grant (T32 GM008505).

References

1. Whiteley M; Diggle SP; Greenberg EP Progress in and Promise of Bacterial Quorum Sensing Research. Nature 2017, 551, 313–320. [PubMed: 29144467]
2. Rutherford ST; Bassler BL Bacterial Quorum Sensing: Its Role in Virulence and Possibilities for Its Control. Cold Spring Harbor Perspect. Med 2012, 2, a012427.
3. Daniels R; Vanderleyden J; Michiels J Quorum Sensing and Swarming Migration in Bacteria. FEMS Microbiol. Rev 2004, 28, 261–289. [PubMed: 15449604]
4. Dickschat JS Quorum Sensing and Bacterial Biofilms. Nat. Prod. Rep 2010, 27, 343–369. [PubMed: 20179876]
5. Zhou J; Yao D; Qian Z; Hou S; Li L; Jenkins ATA; Fan Y Bacteria-Responsive Intelligent Wound Dressing: Simultaneous in Situ Detection and Inhibition of Bacterial Infection for Accelerated Wound Healing. Biomaterials 2018, 161, 11–23. [PubMed: 29421548]
6. Alatraktchi F. A. a.; Noori JS; Tanev GP; Mortensen J; Dimaki M; Johansen HK; Madsen J; Molin S; Svendsen WE Paper-Based Sensors for Rapid Detection of Virulence Factor Produced by Pseudomonas aeruginosa. PloS One 2018, 13, e0194157. [PubMed: 29566025]
7. Kim MK; Zhao A; Wang A; Brown ZZ; Muir TW; Stone HA; Bassler BL Surface-Attached Molecules Control Staphylococcus aureus Quorum Sensing and Biofilm Development. Nat. Microbiol 2017, 2, 17080. [PubMed: 28530651]

8. Broderick AH; Breitbach AS; Frei R; Blackwell HE; Lynn DM Surface-Mediated Release of a Small-Molecule Modulator of Bacterial Biofilm Formation: A Non-Bactericidal Approach to Inhibiting Biofilm Formation in Pseudomonas aeruginosa. Adv. Healthcare Mater 2013, 2, 993–1000.

9. Kratochvil MJ; Welsh MA; Manna U; Ortiz BJ; Blackwell HE; Lynn DM Slippery Liquid-Infused Porous Surfaces That Prevent Bacterial Surface Fouling and Inhibit Virulence Phenotypes in Surrounding Planktonic Cells. ACS Infect. Dis 2016, 2, 509–517. [PubMed: 27626103]

10. Laabei M; Jamieson WD; Massey RC; Jenkins AT A. Staphylococcus aureus Interaction with Phospholipid Vesicles–a New Method to Accurately Determine Accessory Gene Regulator (Agr) Activity. PloS One 2014, 9, e87270. [PubMed: 24498061]

11. Davis B; Richens J; O'shea P Label-Free Critical Micelle Concentration Determination of Bacterial Quorum Sensing Molecules. Biophys. J 2011, 101, 245–254. [PubMed: 21723835]

12. Daniels R; Reynaert S; Hoekstra H; Verreth C; Janssens J; Braeken K; Fauvart M; Beullens S; Heusdens C; Lambrichts I Quorum Signal Molecules as Biosurfactants Affecting Swarming in Rhizobium etli. Proc. Natl. Acad. Sci. U. S. A 2006, 103, 14965–14970. [PubMed: 16990436]

13. Fuqua C; Greenberg EP Listening in on Bacteria: Acyl-Homoserine Lactone Signalling. Nat. Rev. Mol. Cell. Biol 2002, 3, 685–695. [PubMed: 12209128]

14. Schuster M; Lostroh CP; Ogi T; Greenberg EP Identification, Timing, and Signal Specificity of Pseudomonas aeruginosa Quorum-Controlled Genes: A Transcriptome Analysis. J. Bacteriol 2003, 185, 2066–2079. [PubMed: 12644476]

15. Jiang D; Liu Y; Jiang H; Rao S; Fang W; Wu M; Yuan L; Fang W A Novel Screen-Printed Mast Cell-Based Electrochemical Sensor for Detecting Spoilage Bacterial Quorum Signaling Molecules (N-Acyl-Homoserine-Lactones) in Freshwater Fish. Biosens. Bioelectron 2018, 102, 396–402. [PubMed: 29174973]

16. Das S; Sarkar HS; Uddin MR; Mandal S; Sahoo P A Chemosensor to Recognize N-Acyl Homoserine Lactone in Bacterial Biofilm. Sens. Actuators, B 2018, 259, 332–338.

17. Baldrich E; Munoz FX; García-Aljaro C Electrochemical Detection of Quorum Sensing Signaling Molecules by Dual Signal Confirmation at Microelectrode Arrays. Anal. Chem 2011, 83, 2097–2103. [PubMed: 21323339]

18. de Dieu Habimana J; Ji J; Pi F; Karangwa E; Sun J; Guo W; Cui F; Shao J; Ntakirutimana C; Sun X A Class-Specific Artificial Receptor-Based on Molecularly Imprinted Polymer-Coated Quantum Dot Centers for the Detection of Signaling Molecules, N-Acyl-Homoserine Lactones Present in Gram-Negative Bacteria. Anal. Chim. Acta 2018, 1031, 134–144. [PubMed: 30119731]

19. O'Connor G; Knecht LD; Salgado N; Strobel S; Pasini P; Daunert S, Whole-Cell Biosensors as Tools for the Detection of Quorum-Sensing Molecules: Uses in Diagnostics and the Investigation of the Quorum-Sensing Mechanism In Bioluminescence: Fundamentals and Applications in Biotechnology-Volume 3, Springer: 2015; pp 181–200.

20. Patel NM; Moore JD; Blackwell HE; Amador-Noguez D Identification of Unanticipated and Novel N-Acyl L-Homoserine Lactones (Ahls) Using a Sensitive Non-Targeted Lc-Ms/Ms Method. PloS One 2016, 11, e0163469. [PubMed: 27706219]

21. May AL; Eisenhauer ME; Coulston KS; Campagna SR Detection and Quantitation of Bacterial Acylhomoserine Lactone Quorum Sensing Molecules Via Liquid Chromatography–Isotope Dilution Tandem Mass Spectrometry. Anal. Chem 2012, 84, 1243–1252. [PubMed: 22235749]

22. Charlton TS; De Nys R; Netting A; Kumar N; Hentzer M; Givskov M; Kjelleberg S A Novel and Sensitive Method for the Quantification of N-3-Oxoacyl Homoserine Lactones Using Gas Chromatography–Mass Spectrometry: Application to a Model Bacterial Biofilm. Environ. Microbiol 2000, 2, 530–541. [PubMed: 11233161]

23. Barth C; Jakubczyk D; Kubas A; Anastassacos F; Brenner-Weiss G; Fink K; Schepers U; Bräse S; Koelsch P Interkingdom Signaling: Integration, Conformation, and Orientation of N-Acyl-L-Homoserine Lactones in Supported Lipid Bilayers. Langmuir 2012, 28, 8456–8462. [PubMed: 22568488]

24. Toyofuku M; Morinaga K; Hashimoto Y; Uhl J; Shimamura H; Inaba H; Schmitt-Kopplin P; Eberl L; Nomura N Membrane Vesicle-Mediated Bacterial Communication. ISME J 2017, 11, 1504–1509. [PubMed: 28282039]

25. Davis BM; Jensen R; Williams P; O'Shea P The Interaction of N-Acylhomoserine Lactone Quorum Sensing Signaling Molecules with Biological Membranes: Implications for Inter-Kingdom Signaling. PloS One 2010, 5, e13522. [PubMed: 20975958]
26. Sivakumar S; Wark KL; Gupta JK; Abbott NL; Caruso F Liquid Crystal Emulsions as the Basis of Biological Sensors for the Optical Detection of Bacteria and Viruses. Adv. Funct. Mater 2009, 19, 2260–2265.
27. Miller DS; Wang X; Buchen J; Lavrentovich OD; Abbott NL Analysis of the Internal Configurations of Droplets of Liquid Crystal Using Flow Cytometry. Anal. Chem 2013, 85, 10296–10303. [PubMed: 24079265]
28. Lin I-H; Miller DS; Bertics PJ; Murphy CJ; De Pablo JJ; Abbott NL Endotoxin-Induced Structural Transformations in Liquid Crystalline Droplets. Science 2011, 332, 1297–1300. [PubMed: 21596951]
29. Miller DS; Abbott NL Influence of Droplet Size, Ph and Ionic Strength on Endotoxin-Triggered Ordering Transitions in Liquid Crystalline Droplets. Soft Matter 2013, 9, 374–382. [PubMed: 23675387]
30. Carter MC; Miller DS; Jennings J; Wang X; Mahanthappa MK; Abbott NL; Lynn DM Synthetic Mimics of Bacterial Lipid a Trigger Optical Transitions in Liquid Crystal Microdroplets at Ultralow Picogram-Per-Milliliter Concentrations. Langmuir 2015, 31, 12850–12855. [PubMed: 26562069]
31. Carlton RJ; Zayas-Gonzalez YM; Manna U; Lynn DM; Abbott NL Surfactant-Induced Ordering and Wetting Transitions of Droplets of Thermotropic Liquid Crystals "Caged" inside Partially Filled Polymeric Capsules. Langmuir 2014, 30, 14944–14953. [PubMed: 24911044]
32. Chang C-Y; Chen C-H Oligopeptide-Decorated Liquid Crystal Droplets for Detecting Proteases. Chem. Commun 2014, 50, 12162–12165.
33. Alino VJ; Pang J; Yang K-L Liquid Crystal Droplets as a Hosting and Sensing Platform for Developing Immunoassays. Langmuir 2011, 27, 11784–11789. [PubMed: 21863867]
34. Gupta JK; Sivakumar S; Caruso F; Abbott NL Size-Dependent Ordering of Liquid Crystals Observed in Polymeric Capsules with Micrometer and Smaller Diameters. Angew. Chem., Int. Ed 2009, 48, 1652–1655.
35. Kinsinger MI; Buck ME; Abbott NL; Lynn DM Immobilization of Polymer-Decorated Liquid Crystal Droplets on Chemically Tailored Surfaces. Langmuir 2010, 26, 10234–10242. [PubMed: 20405867]
36. Guo X; Manna U; Abbott NL; Lynn DM Covalent Immobilization of Caged Liquid Crystal Microdroplets on Surfaces. ACS Appl. Mater. Interfaces 2015, 7, 26892–26903. [PubMed: 26562466]
37. Sivakumar S; Gupta JK; Abbott NL; Caruso F Monodisperse Emulsions through Templating Polyelectrolyte Multilayer Capsules. Chem. Mater 2008, 20, 2063–2065.
38. Miller MB; Bassler BL Quorum Sensing in Bacteria. Ann. Rev. Microbiol 2001, 55, 165–199. [PubMed: 11544353]
39. Churchill ME; Chen L Structural Basis of Acyl-Homoserine Lactone-Dependent Signaling. Chem. Rev 2010, 111, 68–85. [PubMed: 21125993]
40. Yates EA; Philipp B; Buckley C; Atkinson S; Chhabra SR; Sockett RE; Goldner M; Dessaux Y; Cámara M; Smith H N-Acylhomoserine Lactones Undergo Lactonolysis in a Ph-, Temperature-, and Acyl Chain Length-Dependent Manner During Growth of Yersinia pseudotuberculosis and Pseudomonas aeruginosa. Infect. Immun 2002, 70, 5635–5646. [PubMed: 12228292]
41. Deziel E; Lepine F; Milot S; Villemur R Rhla Is Required for the Production of a Novel Biosurfactant Promoting Swarming Motility in Pseudomonas aeruginosa: 3-(3-Hydroxyalkanoyloxy) Alkanoic Acids (Haas), the Precursors of Rhamnolipids. Microbiology 2003, 149, 2005–2013. [PubMed: 12904540]
42. Miller DS; Carlton RJ; Mushenheim PC; Abbott NL Introduction to Optical Methods for Characterizing Liquid Crystals at Interfaces. Langmuir 2013, 29, 3154–3169. [PubMed: 23347378]

43. Lockwood NA; Abbott NL Self-Assembly of Surfactants and Phospholipids at Interfaces between Aqueous Phases and Thermotropic Liquid Crystals. Curr. Opin. Colloid Interface Sci 2005, 10, 111–120.
44. Uline MJ; Meng S; Szleifer I Surfactant Driven Surface Anchoring Transitions in Liquid Crystal Thin Films. Soft Matter 2010, 6, 5482–5490.
45. Zhong S; Jang C-H Ph-Driven Adsorption and Desorption of Fatty Acid at the Liquid Crystal–Water Interface. Liq. Cryst 2016, 43, 361–368.
46. Brake JM; Mezera AD; Abbott NL Effect of Surfactant Structure on the Orientation of Liquid Crystals at Aqueous− Liquid Crystal Interfaces. Langmuir 2003, 19, 6436–6442.
47. Tan LN; Carlton R; Cleaver K; Abbott NL Liquid Crystal-Based Sensors for Rapid Analysis of Fatty Acid Contamination in Biodiesel. Mol. Cryst. Liq. Cryst 2014, 594, 42–54.
48. Porter D; Savage JR; Cohen I; Spicer P; Caggioni M Temperature Dependence of Droplet Breakup in 8CB and 5CB Liquid Crystals. Phys. Rev. E 2012, 85, 041701.
49. Pearson JP; Pesci EC; Iglewski BH Roles of Pseudomonas aeruginosa Las and Rhl Quorum-Sensing Systems in Control of Elastase and Rhamnolipid Biosynthesis Genes. J. Bacteriol 1997, 179, 5756–5767. [PubMed: 9294432]
50. Smalley NE; An D; Parsek MR; Chandler JR; Dandekar AA Quorum Sensing Protects Pseudomonas aeruginosa against Cheating by Other Species in a Laboratory Coculture Model. J. Bacteriol 2015, 197, 3154–3159. [PubMed: 26195596]
51. Jacobs MA; Alwood A; Thaipisuttikul I; Spencer D; Haugen E; Ernst S; Will O; Kaul R; Raymond C; Levy R Comprehensive Transposon Mutant Library of Pseudomonas aeruginosa. Proc. Natl. Acad. Sci. U. S. A 2003, 100, 14339–14344. [PubMed: 14617778]
52. Geske GD; O'Neill JC; Miller DM; Mattmann ME; Blackwell HE Modulation of Bacterial Quorum Sensing with Synthetic Ligands: Systematic Evaluation of N-Acylated Homoserine Lactones in Multiple Species and New Insights into Their Mechanisms of Action. J. Am. Chem. Soc 2007, 129, 13613–13625. [PubMed: 17927181]
53. Moore JD; Rossi FM; Welsh MA; Nyffeler KE; Blackwell HE A Comparative Analysis of Synthetic Quorum Sensing Modulators in Pseudomonas aeruginosa: New Insights into Mechanism, Active Efflux Susceptibility, Phenotypic Response, and Next-Generation Ligand Design. J. Am. Chem. Soc 2015, 137, 14626–14639. [PubMed: 26491787]
54. Clasquin MF; Melamud E; Rabinowitz JD Lc-Ms Data Processing with Maven: A Metabolomic Analysis and Visualization Engine. Curr. Protoc. Bioinf 2012, 37, 14.11. 1–14.11. 23.
55. Mata-Sandoval JC; Karns J; Torrents A Effect of Nutritional and Environmental Conditions on the Production and Composition of Rhamnolipids by P. aeruginosa Ug2. Microbiological research 2001, 155, 249–256. [PubMed: 11297354]
56. Zhao F; Shi R; Ma F; Han S; Zhang Y Oxygen Effects on Rhamnolipids Production by Pseudomonas aeruginosa. Microbial cell factories 2018, 17, 39. [PubMed: 29523151]
57. Abdel-Mawgoud AM; Lépine F; Déziel E Rhamnolipids: Diversity of Structures, Microbial Origins and Roles. Applied microbiology and biotechnology 2010, 86, 1323–1336. [PubMed: 20336292]
58. Miller DS; Wang X; Buchen J; Lavrentovich OD; Abbott NL Analysis of the Internal Configurations of Droplets of Liquid Crystal Using Flow Cytometry. Analytical chemistry 2013, 85, 10296–10303. [PubMed: 24079265]
59. Holloway B Genetic Recombination in Pseudomonas aeruginosa. Microbiology 1955, 13, 572–581.
60. Welsh MA; Eibergen NR; Moore JD; Blackwell HE Small Molecule Disruption of Quorum Sensing Cross-Regulation in Pseudomonas aeruginosa Causes Major and Unexpected Alterations to Virulence Phenotypes. Journal of the American Chemical Society 2015, 137, 1510–1519. [PubMed: 25574853]

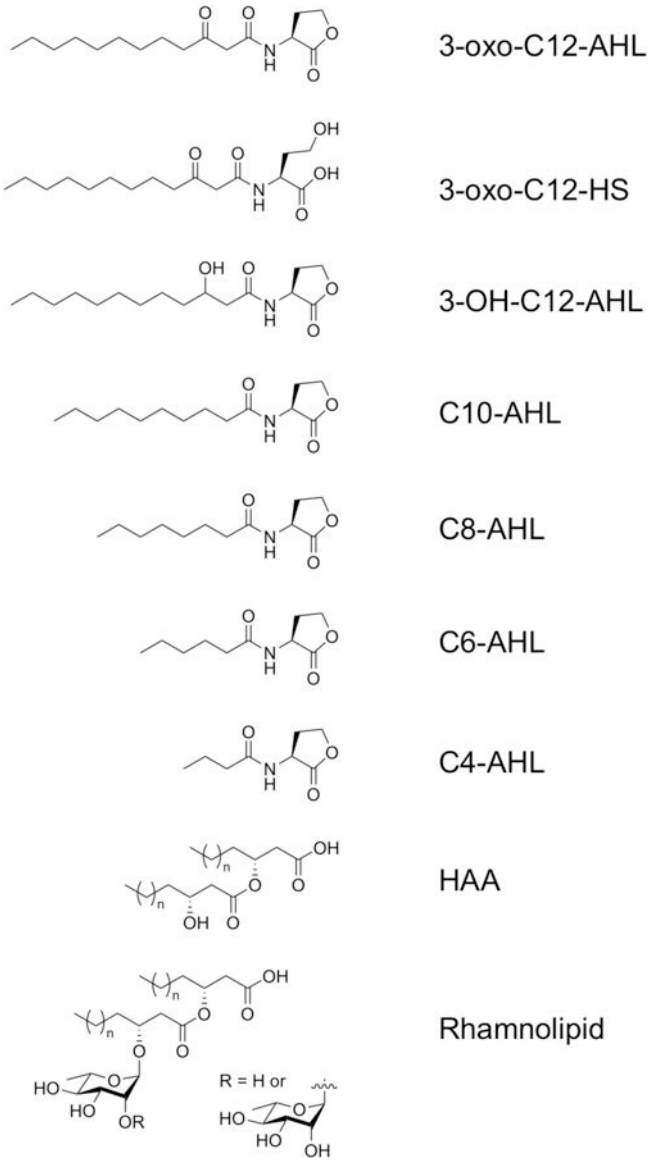

Figure 1.

Structures of the AHLs and bacterial biosurfactants investigated in this study (n = 3–11 for rhamnolipid and HAA). HAA was evaluated as a mixture of stereoisomers; see SI.

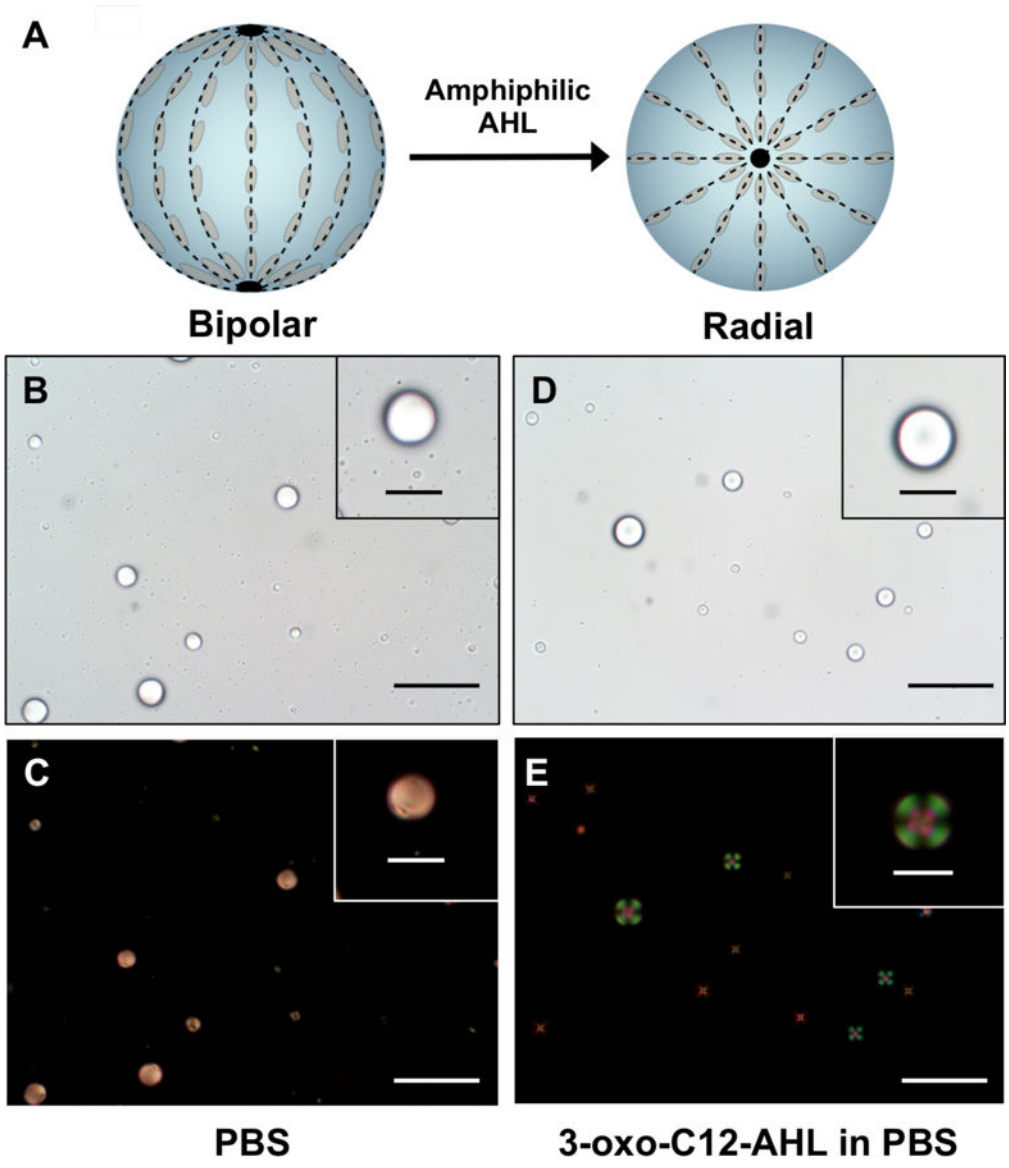

Figure 2.

A) Schematic of the LC director profiles (dotted lines) for spherical LC droplets in the bipolar (left) and radial (right) states. Black points represent characteristic defects associated with each state. B-C and D-E show bright-field (B, D) and polarized-light (C, E) micrographs of 5CB droplets in the bipolar (B-C) and radial (D-E) states. B-C) Images of LC droplets dispersed in PBS. D-E) Images of LC droplets dispersed in PBS after the addition of 3-oxo-C12 AHL (50 μM). Droplets in (C) and (E) were imaged using crossed polarizers oriented parallel to the 30 μm scale bars in the main image (scale bars = 10 μm for insets).

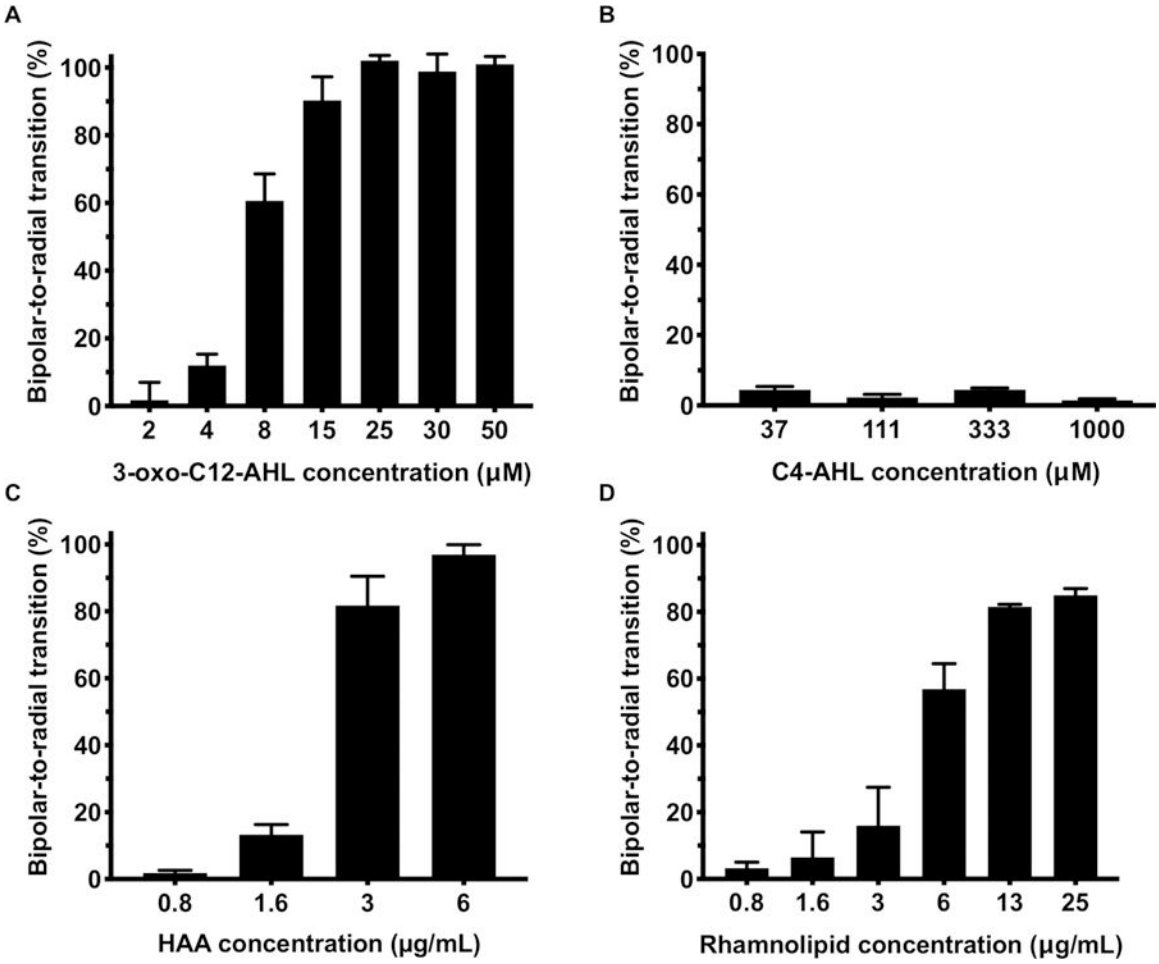

Figure 3.

(A-C) Plots showing the percentage of LC droplets transformed from bipolar to radial as a function of the concentration of A) 3-oxo-C12-AHL, B) C4-AHL, and C) HAA in PBS containing 1% v/v DMSO. (D) Plot showing the percentage of LC droplets transformed as a function of rhamnolipid concentration. Data represents the mean ± SEM (n = 4).

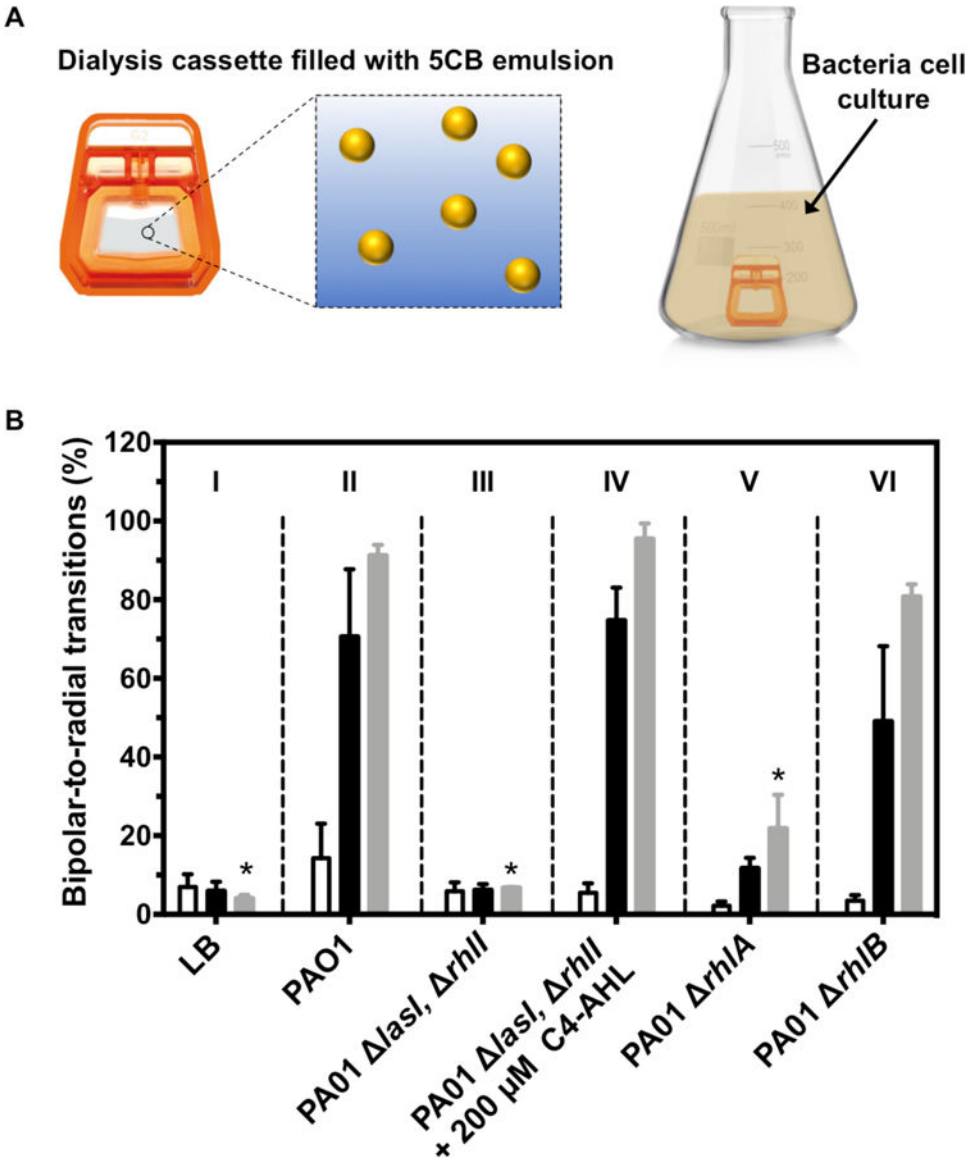

Figure 4.

(A) Schematic showing experimental set up used to incubate LC emulsions with bacterial cultures using dialysis cassettes. (B) Plot showing percentage of LC droplets transformed from bipolar to radial after 90 min of incubation with cultures grown at 37 °C for 6 h (white bars), 12 h (black bars), and 24 h (grey bars). Columns I–VI show results using an LB medium control (I) or using the bacterial strains and conditions indicated. Results are the average of 3 independent experiments; error bars represent SEM. Asterisk (*) indicates $p < 0.05$ for multiple comparisons of each group against group II (PAO1) at the 24-hour time point.

Table 1.

BR_{50} values for AHLs, rhamnolipids, and HAA.[a]

Amphiphile	BR_{50} Value (μM)[a]	95% CI (μM)
3-oxo-C12-AHL	7.1	6.7–7.6
3-oxo-C12-HS	20	14–29
3-OH-C12-AHL	16	13–20
C10-AHL	>72	–
C8-AHL	>360	–
C6-AHL	–	–
C4-AHL	–	–
HAA	2.3 μg/mL (8 μM)	2.1–2.5 μg/mL
Rhamnolipids	5.9 μg/mL (~7–20 μM)[b]	5.1–6.9 μg/mL

[a] BR_{50} is defined as the minimum concentration required to induce changes from bipolar to radial states in at least a 50% of LC droplets. Values were obtained from sigmoidal regressions to the data plotted in Figures 3 and S2. CI = confidence interval.

[b] We estimate the molar concentration of a 6 μg/mL mixture of commercial rhamnolipids to be in this micromolar range; see SI for additional details.